Aalborg Universitet

Model Reference Adaptive Control of UIPC in Islanded Hybrid Microgrids with Flexible Loads and Storages

Zolfaghari, Mahdi ; Gharehpetian, Gevork B. GHAREHPETIAN; Blaabjerg, Frede; Anvari-Moghaddam, Amjad

Model Reference Adaptive Control of UIPC in Islanded Hybrid Microgrids with Flexible Loads and Storages

Mahdi Zolfaghari
Power System Secure Operation
Research Centre
Amirkabir University of Technology
Tehran, Iran
mahdizolfaghari@aut.ac.ir

Gevork. B. Gharehpetian
Electrical Engineering Department
Amirkabir University of Technology
Tehran, Iran
grptian@aut.ac.ir

Frede Blaabjerg
Department of Energy
Aalborg University
Aalborg, Denmark
fbl@energy.aau.dk

Amjad Anvari-Moghaddam
Department of Energy
Aalborg University
Aalborg, Denmark
aam@energy.aau.dk

Abstract—**The islanding operation of hybrid microgrids (HmGs), which adopt the unified interphase power controller (UIPC) as the major element for interconnecting of AC and DC subsystems, is analyzed in this work. The studied HmG includes two AC subsystems and one energy storage-based DC subsystem (ESDC) and some flexible loads. A model reference adaptive control (MRAC) mechanism is suggested to control the UIPC, maintaining an appropriate bidirectional power flow control with simple structure. As another contribution, a new structure topology for the UIPC's power converter at DC side is proposed based on the dual-active-bridge topology and a harmonic-based modeling approach is follow-up for UIPC's power converter modelling. The results of simulations indicate acceptable islanding operation performance of HmG with the proposed structure.**

Keywords—Hybrid microgrid, UIPC, MRAC, flexible load

I. INTRODUCTION

In obedience to the literature, hybrid microgrids (HmGs) are good choice to interconnected multiple AC and DC subsystems since they reduce the AC/DC conversion stages, provide general management of several AC and DC subsystems, and facilitate the integration of these subsystems with current power grid [1, 2]. The HmGs mainly encompass several AC and DC subsystems which have commonly been tied together through several power converters with parallel connection. The interconnection of these subsystems is essential since it provides the subsystem the capability to transfer power during emergencies and as result, the stability and security of the subsystems are preserved [3-7]. Nevertheless, adopting the parallel converters brings numerous challenges to the control and operation of HmGs; to name a few, circulating current, output voltage magnitude and phase equalization, appropriate power sharing etc. to address these issues, tens of research studies have been presented in the literature. For example, in [8], a Γ-Z-Source single power converter has been presented to interconnect HmGs. The authors of [9] Γ-Z-Source have developed the method of [8] into parallel-connected Γ-Z-Source power converters for HmGs. This way, the exchange power between the subsystems is increased and the system reliability is also increased [9]. In [10], a topology for the interlink converter has been proposed which enables the DC link to integrate a storage system. Thus, the power and DC link voltage

oscillations are relieved. In [11], conventional droop concept has been developed to control the power converters in HmGs. Further, the authors of [12] have used the virtual droop concept to improve the power sharing performance of interlink power converters in HmGs.

More recently, the UIPC has been proposed as an effective alternative to the parallel interlink power converters to interconnect HmGs. In [13], the UIPC has been implemented to interconnected two AC subsystems and one DC subsystem. The HmG, as a whole system, has been connected to upstream grid and the power exchange between the subsystems as well as with the upstream grid has been analyzed. The upstream grid has been responsible for regulating frequency and voltage in HmG and the UIPC has been controlled such that stable power exchange among the subsystems preserved. Furthermore, the interconnection of a greater number of AC and DC subsystems using UIPC has been investigated in [7] where the studied HmG has been tied to the upstream power system.

Yet, the islanding operation of HmG interconnected by UIPC has not been investigated, to the best of the authors' knowledge. Therefore, this work aims at studying the islanding operation of HmG. A new structure for the UIPC's power converter at the DC side is proposed based on the dual-active-bridge topology and a new control scheme for the UIPC, based on a model reference adaptive control (MRAC) concept, is developed afterwards. The harmonic-based modeling approach has been applied to model the DC side power converter to simplify the control design process.

The rest of this paper is organized as follows: Section II presents the dynamic model of the studied HmG and new structure of UIPC. The proposed MRAC-based control of UIPC is described in Section III. The simulation results are given in Section IV and at last, concluding remarks are drawn in Section V.

II. SYSTEM MODEL AND PROPOSED UIPC TOPOLOGY

As demonstrated in Fig. 1, a typical HmG including two AC subsystems and an energy storage-based DC subsystem (ESDC) is considered in this study. The HmG operates in islanded mode and AC mG1, AC mG2, and ESDC are interconnected through UIPC. AC mG1 includes an energy

storage system (ESS), a wind turbine, and flexible and non-flexible loads. AC mG2 contains a PV system which is connected to the AC common bus through DC/DC and DC/AC power conversion units. An ESS and a non-flexible load also exist in this subsystem. The ESDC includes a group of ESSs which can be simultaneously charged/discharged. There is also an energy management system (EMS) which controls and monitors the whole HmG operating conditions such as voltage, frequency of AC subsystems, and exchange power between subsystems. The ESDC is able to provide bidirectional DC power flow, i.e., the ESSs in the ESDC can be charged/discharged when necessary. It is important to note that there is a flexible load in AC mG1 which can increase/decrease its power consumption based on operating condition and generated reference signal from UIPC and EMS. The details are given in the next section.
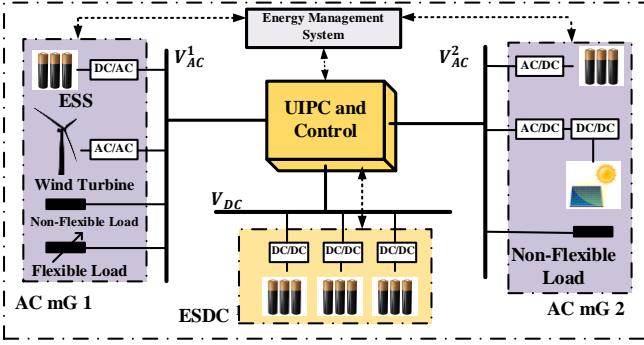

Fig. 1. Structure of studied HmG which is interconnected by UIPC

A. Proposed UIPC Topology

To adopt the ESDC into the HmG structure through the UIPC, we propose a new configuration for the UIPC's power converter at DC side, as shown in Fig. 2. The indicated per-phase model includes two main parts: series power converter (SPC) and parallel power converter (PPC). The main task of SPC is to inject an adjustable series voltage through power transformer T_{SPC} into the transmission line to control the power flow between the two AC buses, i.e., V_{AC}^1 and V_{AC}^2. Each phase of the UIPC has one SPC, indexed by SPC_i, $i = 1,2,3$. The PPC aims on regulating the DC side voltage as well as V_{AC}^1. It also controls the bidirectional power flow in coordination with the ESSs main power converters (MC) which connects all ESSs to the UIPC DC bus. The MC accompanied by the voltage multiplier and the high-frequency transformer (HFT) constitute a dual-active-bridge topology. The MC is connected to the ESDC subsystem directly and is to be controlled through the MRAC strategy, as will be discussed in the next section. The HFT accomplishes two main duties; 1) providing galvanic voltage isolation, and 2) increasing boosting coefficient of the conversion stages with reduced cost. However, if not controlled appropriately, the efficiency of this system may be reduced due to circulating current. Thus, to avoid this problem, the MRAC is proposed in this study. It should be mentioned that the UIPC has only one PPC for all phases. The UIPC acts in two modes; capacitive or inductive. The bidirectional switches S_1 and S_2 are commanded based on the UIPC operation mode to allow correct power flow direction.
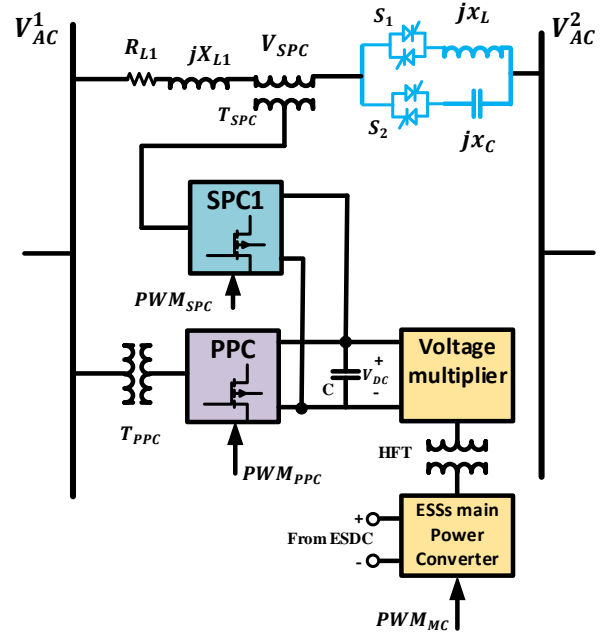

Fig. 2. Proposed UIPC topology

B. Reduced Order Model of Dual-Active Bridge Conversion Stage and Harmonic-based Modelling

To design the MRAC controller, the dynamics of the plant should be determined first. The voltage multiplier circuit of Fig. 2 is a three-phase neutral point-clamped (NPC) power converter which is connected to the secondary side of HFT. This circuit multiplies the output voltage of MC by 2 in order to reduce the ratio of HFT windings. For the PPC, a three-phase full-bridge NPC with bidirectional switches is considered. All the switches in the MC and voltage multiplier circuit are also bidirectional since the whole DC side should be able to provide bidirectional power flow. The square pulse of half duty cycle control method has been applied to produce the voltages V_p and V_s, which is the voltage across the primary and secondary windings of the HFT, respectively, which have been shifted by γ in relation to the power flow direction. The exchanged power is given by:

$$P_{ex} = a_N \left(\left(V_p V_s \gamma (\pi - |\gamma|) \right) \Big/ 2\pi \omega L_1 \right) \tag{1}$$

where a_N is the ration of HFT and L_1 is the inductance of the line and between HTF and output of MC. Fig. 3 illustrates the voltages and input current of HTF considered in the modelling process based on (1).

Supposing instantaneous switching functions for all bidirectional switches, a harmonic-based model can be reached by applying Fourier transformation to the switching function of the dual-bridge conversion stage as follows:

$$S(t) = 1/2 +$$
$$2/\pi \left(\sum_{k=0}^{\infty} \left(\sin((2k+1)(\omega_s t - \varphi_j)) \right) \Big/ (2k+1) \right), j = 1, \dots, 4 \tag{2}$$
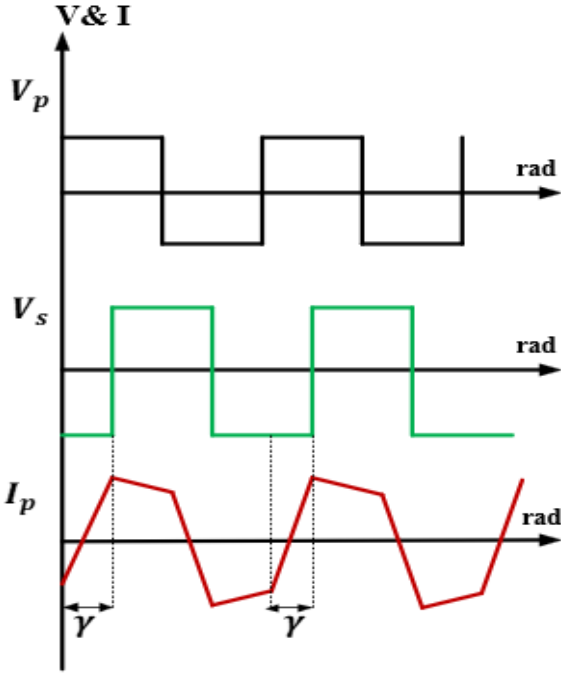
Fig. 3. Primary and secondary voltages, and primary current of HFT

where ω_s is the switching frequency in rad/s and φ_j is the lateness of the pulse w.r.t the desired reference frame. Considering the switching function (2), the voltages V_p and V_s can be written as follows:

$$V_p\big(S(t)\big) = V_{ESDC}[S_1(t) - S_2(t)] \tag{3}$$

$$V_s\big(S(t)\big) = \frac{V_{DC}}{2}[S_3(t) - S_4(t)] \tag{4}$$

The duty cycle is 0.5 in the modelling process w.r.t the square wave switching pulses. Therefore, $S_2(t)$ is the complement of $S_1(t)$ and we have $\varphi_2 = \pi + \varphi_1$, and in the same way, $\varphi_4 = \pi + \varphi_3$. Also, forcing $\varphi_1 = 0$ then $\varphi_3 = \gamma$. Accordingly, (3) and (4) become:

$$V_p(t) = V_{ESDC}\left(\frac{4}{\pi}\left(\sum_{k=0}^{\infty} \frac{sin((2k+1)\omega_s t)}{(2k+1)}\right)\right) \tag{5}$$

$$V_s(t) = \frac{V_{DC}}{2}\left(\frac{4}{\pi}\left(\sum_{k=0}^{\infty} \frac{sin((2k+1)\omega_s t - \gamma)}{(2k+1)}\right)\right) \tag{6}$$

According to Kirchhoff's voltage law, in the primary winding of HFT one obtains:

$$V_p(t) - a_N V_s(t) = R_1 I_p + L_1 \frac{dI_p(t)}{dt} =$$
$$V_{ESDC}\left(\frac{4}{\pi}\left(\sum_{k=0}^{\infty} \frac{sin((2k+1)\omega_s t)}{(2k+1)}\right)\right) -$$
$$\frac{a_N V_{DC}}{2}\left(\frac{4}{\pi}\left(\sum_{k=0}^{\infty} \frac{sin((2k+1)\omega_s t - \gamma)}{(2k+1)}\right)\right) \tag{7}$$

Solving (7) for $I_p(t)$ gives:

$$I_p(t) = \frac{4}{\pi}\sum_{k=0}^{\infty} \frac{1}{(2k+1)}\left(\frac{V_{ESDC}}{z(k)} sin\big((2k+1)\omega_s t - \varphi_{z(k)}\big) - \frac{a_N V_{DC}}{2|z(k)|} sin\big((2k+1)\omega_s t - \varphi_{z(k)}\big)\right) \tag{8}$$

where $|z(k)| = \left(R_1^2 + \big((2k+1)\omega_s L_1\big)^2\right)^{1/2}$ and $\varphi_{z(k)} = tan^{-1}\left(\frac{(2k+1)\omega_s L_1}{R_1}\right)$.

According to Kirchhoff's current law, the current of output capacitor is as follows:

$$\frac{C}{2}\frac{dV_{DC}}{dt} = I_s - I_{dc} = a_N I_p[S_3(t) - S_4(t)] - \frac{V_{DC}}{R_{out}} \tag{9}$$

Rearranging and simplifying (9) we obtain:

$$\frac{d}{dt}(V_{DC}) = h(V_{DC}(t), \gamma) = \frac{16 a_N}{C\pi^2}\left(\sum_{k=0}^{\infty} \frac{1}{(2k+1)^2}\left(\frac{V_{ESDC}}{z(k)} cos\big((2k+1)\gamma - \varphi_{z(k)}\big) - \frac{a_N V_{DC}}{|z(k)|} cos\big(\varphi_{z(k)}\big)\right)\right) - \frac{2V_{DC}}{CR_{out}} \tag{10}$$

Since usually $\omega_s L_1 \gg R_1$, thus, $\varphi_{z(k)} \cong \frac{\pi}{2}$. Therefore, we can write:

$$\frac{d}{dt}(V_{DC}) = h\big(V_{DC}(t)\big) + Qu \tag{11}$$

In which $h\big(V_{DC}(t)\big) = \frac{-2V_{DC}}{CR_{out}} = -\rho V_{DC}$, $Q = \frac{16 a_N}{C\pi^2}\left(\sum_{k=0}^{\infty} \frac{1}{(2k+1)^2}\left(\frac{V_{ESDC}}{z(k)}\right)\right)$, and $u = sin\big((2k+1)\gamma\big)$. Therefore, we use this first order transfer function to design the controller in the next section.

III. PROPOSED MRAC-BASED CONTROL OF UIPC

In each subsystem, some important operational parameters should be controlled so that the overall HmG keeps stable operation. Since the HmG operate in islanded mode, in the AC subsystems, the voltage and frequency should be maintained in operational limits while the DC link voltage in the ESDC subsystem should be kept in stable region. In this section a new control structure for the UIPC and HmG management is proposed. The MRAC-based control scheme for the DC side is also presented.

A. General Structure of Proposed HmG management System and Control of UIPC

Per-phase model of proposed UIPC control scheme and HmG management system is illustrated in Fig. 4. As shown, three control units are considered for the power converters of the UIPC system. More importantly, there is an energy management system which monitors the status of the subsystems; performing essential reference signal calculations for the subsystems based on the feedbacks from the subsystems and user-defined reference points.
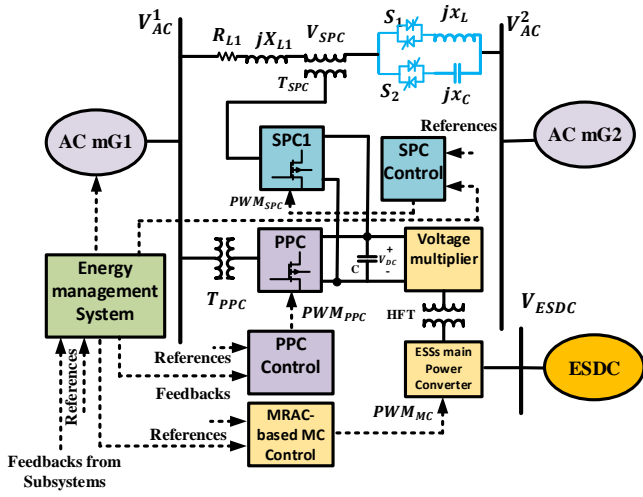
Fig. 4. Proposed UIPC control structure and HmG management system

B. MRAC-based Controller Design

The proposed MRAC control scheme is represented in Fig. 5. As shown, a reference model is used to generate the reference output $y_{ref}(t)$ according to reference input $u_{ref}(t)$. The error $e_y(t)$ is given to the adaptation control law to estimate $\mathcal{F}_{ref}$ and $\mathcal{F}_p$. Then, the controller generates the control signal $u(t)$ which is applied to the MC plant.

In contrast to the dynamic plant described by (11), the dynamics of reference model are as follows:

$$\frac{d}{dt}\big(y_{ref}(t)\big) = -\mathcal{F}_{ref}y_{ref}(t) + B_{ref}u_{ref}(t) \qquad (12)$$

where $\mathcal{F}_{ref}$ and B_{ref} are non-negative real constants, and $y_{ref}(t)$ and $u_{ref}(t)$ are respectively the DC link voltage variation and voltage oscillation limit. For the real dynamic model, ΔV_{DC} is supposed to be the system output $y(t)$. The droop characteristic for the DC voltage is demonstrated in Fig. 6 where $P_{ESS,Nom}$ is the nominal power value of ESSs in charging/discharging process, $V_{DC,Nom}$ is the nominal value of DC link voltage, and α_{dp} is the droop coefficient. For the positive power low direction, the DC link voltage drops whereas it increases for the negative power flow direction. Thus, the droop pattern lets to control the power exchange while keeping the DC link voltage stable.
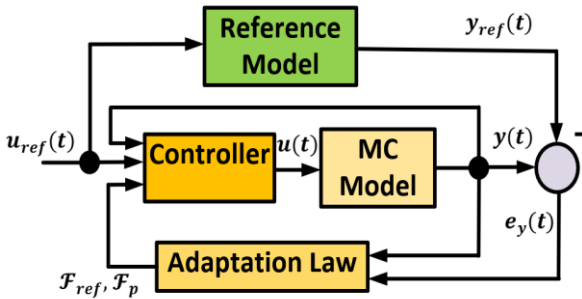

Fig. 5. Proposed MRAC control of MC converter

In the MRAC, the difference between $y_{ref}(t)$ and $y(t)$ is forced to zero by choosing the appropriate control law as follows:

$$u(t) = \mathcal{F}_{ref}u_{ref}(t) + \mathcal{F}_p y(t) \qquad (13)$$

where $\mathcal{F}_{ref}$ and $\mathcal{F}_p$ are time-varying parameters which are approximated by the adaptation law as follows:

$$\frac{d}{dt}\big(\mathcal{F}_{ref}(t)\big) = -sign(Q)\mu e_y(t)\, u_{ref}(t) \qquad (14)$$

$$\frac{d}{dt}\big(\mathcal{F}_p(t)\big) = -sign(Q)\mu e_y(t)\, y(t) \qquad (15)$$
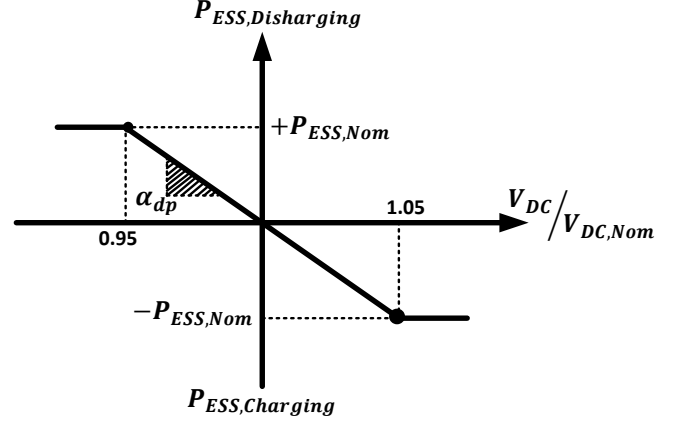
where μ is a real positive value.

Fig. 6. Droop characteristic in the proposed control scheme

IV. SIMULATION RESULTS

To verify the performance of the proposal described in this work, simulation results using MATLAB/SIMULINK are provided here. The HmG illustrated in Fig. 1 is considered for the simulation which includes two AC subsystems and one ESDC. AC mG1 contains a wind turbine generating system with nominal power of $150kW$ which has been provided by three $50kW$ units ($3 \times 50\ kW$). There is a $50kW$ battery ESS in this mG. Also, one flexible load and one non-flexible load are connected to the common AC bus of AC mG1. A PV system with nominal power of $250kW$, a $50kW$ battery ESS, and one non-flexible load are included in AC mG2. The ESDC also contains three $50kW$ battery ESSs which can provide bidirectional DC power flow through the dual-bridge structure with proposed MRAC-based control strategy.

In AC mG1, the nominal power of the non-flexible load is $160kW$. The total power provided by the wind units is $150kW$; therefore, the battery ESS in this mG is also discharged to meet the demand. However, a flexible load with consumption characteristic as $20\ kW : 20\ kW : 80\ kW$ can respond to the extra power provided by the battery and use it, possibly based on the contraction between the flexible load owner and power market operator. Therefore, as shown in Fig. 7, the power consumption in AC mG1, at t = 0.4s, increases from $180kW$ to $200kW$. Further, Fig. 8 shows the response of the flexible load to the UIPC reference signal. As it is clear, the load has been successfully able to increase its consumption from $20kW$ to $40kW$. Fig. 9 shows the state of charge (SOC) of the battery in AC mG1. As it is clear, before t = 0.4s the battery discharging is been initiated since the wind units were not able to support the extra $30kW$ load power ($20kW$ of base power of flexible load+$10kW$ of the non-flexible load). At t = 0.4s, the flexible load is commanded by the UIPC to increase its consumption by $20kW$. Thus, as can be seen from Fig. 9, the rate of discharge is increased. The DC link voltage of UIPC in this situation is also illustrated in Fig. 10. As shown, the DC link

control has successfully been able to handle the oscillations and stabilizes the DC link voltage at its nominal value 480V.
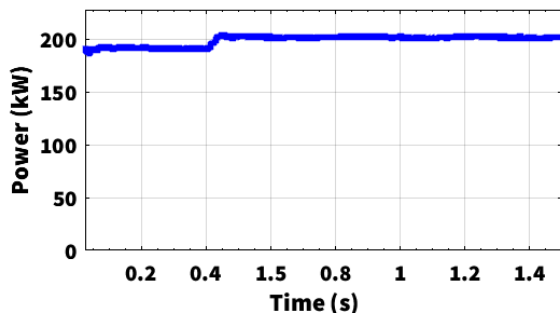

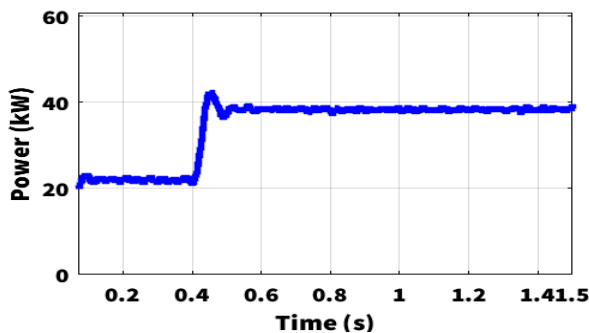Fig. 7. Power consumption in AC mG1 when the flexible load changes its consumption at t = 0.4s.

Fig. 8. Power consumption by flexible load changes at t = 0.4s.

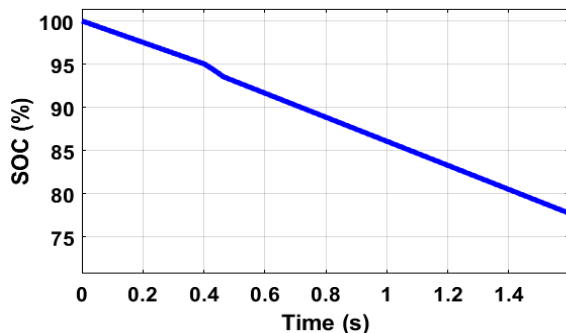

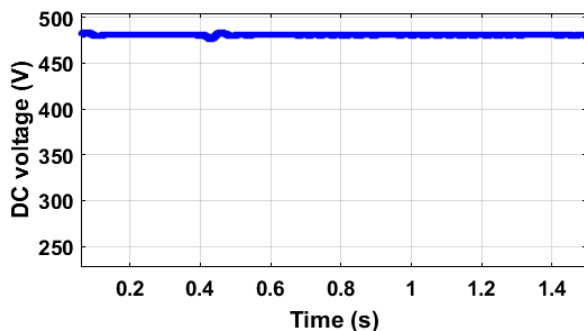Fig. 9. State of charge of battery in AC mG1 when the flexible load changes its consumption at t = 0.4s.

Fig. 10. DC link voltage of UIPC the flexible load changes its consumption at t = 0.4s.

V. CONCLUSION

The HmGs are alleged to be the mostly used base structure to embed the DC and AC resources and loads in smart grids. These microgrids have traditionally been interconnected using bidirectional power converters. However, recently, the UIPC, in place of power converters, has been presented in literature to interconnect HmGs. Nevertheless, the islanding operation of UIPC-based HmGs has not been studied in literature. This work filled this research gap and further proposed a new MRAC-based control scheme and a new topology for UIPC. The results confirmed that the proposed topology and control scheme for UIPC are useful when interconnecting a HmG using UIPC operating in islanded mode.

REFERENCES

[1] J. Chang, S. Moon, G. Lee, and P. Hwang, "A New Local Control Method of Interlinking Converters to Improve Global Power Sharing in an Islanded Hybrid AC/DC Microgrid," IEEE Transactions on Energy Conversion, pp. 1-1, 2020, doi: 10.1109/TEC.2020.2967416.

[2] M. Zolfaghari, M. Abedi, and G. B. Gharehpetian, "Robust Nonlinear State Feedback Control of Bidirectional Interlink Power Converters in Grid-Connected Hybrid Microgrids," IEEE Systems Journal, vol. 14, no. 1, pp. 1117-1124, 2020, doi: 10.1109/JSYST.2019.2919551.

[3] S. M. Malik, Y. Sun, X. Ai, C. Zhengqi, and J. A. Ansari, "Droop-based Converter Scheme for Linking Multiple Hybrid Microgrids," in 2019 2nd International Conference on Computing, Mathematics and Engineering Technologies (iCoMET), 30-31 Jan. 2019 2019, pp. 1-5, doi: 10.1109/ICOMET.2019.8673415.

[4] F. Wang, J. L. Duarte, and M. A. M. Hendrix, "Grid-Interfacing Converter Systems With Enhanced Voltage Quality for Microgrid Application—Concept and Implementation," IEEE Transactions on Power Electronics, vol. 26, no. 12, pp. 3501-3513, 2011, doi: 10.1109/TPEL.2011.2147334.

[5] M. Zolfaghari, M. Abedi, G. B. Gharehpetian, and J. M. Guerrero, "Flatness-Based Decentralized Control of Bidirectional Interlink Power Converters in Grid-Connected Hybrid Microgrids Using Adaptive High-Gain PI-Observer," IEEE Systems Journal, pp. 1-9, 2020, doi: 10.1109/JSYST.2020.2977660.

[6] M. Zolfaghari, G. B. Gharehpetian, and A. Anvari-Moghaddam, "Quasi-Luenberger Observer-Based Robust DC Link Control of UIPC for Flexible Power Exchange Control in Hybrid Microgrids," IEEE Systems Journal, pp. 1-10, 2020, doi: 10.1109/JSYST.2020.2991653.

[7] M. Zolfaghari, M. Abedi, and G. B. Gharehpetian, "Power Exchange Control of Clusters of Multiple AC and DC Microgrids Interconnected by UIPC in Hybrid Microgrids," in 2019 24th Electrical Power Distribution Conference (EPDC), 19-20 June 2019 2019, pp. 22-26, doi: 10.1109/EPDC.2019.8903809.

[8] M. Poursmaeil, S. M. Dizgah, H. Torkaman, and E. Afjei, "Autonomous control and operation of an interconnected AC/DC microgrid with Γ-Z-Source interlinking converter," in 2017 Smart Grid Conference (SGC), 20-21 Dec. 2017 2017, pp. 1-6, doi: 10.1109/SGC.2017.8308836.

[9] M. B. Mahdi Zolfaghari, G. B. Gharehpetian, "Adaptive Gain-Regulating-based Control of Parallel-Connected Γ-Z-Source Power Converters in Hybrid Microgrids," INTERNATIONAL CONFERENCE ON ENVIRONMENT AND ELECTRICAL ENGINEERING, 2020.

[10] U. Bose, S. Chattopadhyay, and C. Chakraborty, "Topological investigation on interlinking converter in a hybrid microgrid," in 2018 IEEE International Conference on Industrial Electronics for Sustainable Energy Systems (IESES), 31 Jan.-2 Feb. 2018 2018, pp. 62-67, doi: 10.1109/IESES.2018.8349851.

[11] J. Jiao, R. Meng, Z. Guan, C. Ren, L. Wang, and B. Zhang, "Grid-connected Control Strategy for Bidirectional AC-DC Interlinking Converter in AC-DC Hybrid Microgrid," in 2019 IEEE 10th International Symposium on Power Electronics for Distributed Generation Systems (PEDG), 3-6 June 2019 2019, pp. 341-345, doi: 10.1109/PEDG.2019.8807601.

[12] H. Xiao, A. Luo, Z. Shuai, G. Jin, and Y. Huang, "An Improved Control Method for Multiple Bidirectional Power Converters in Hybrid AC/DC Microgrid," IEEE Transactions on Smart Grid, vol. 7, no. 1, pp. 340-347, 2016, doi: 10.1109/TSG.2015.2469758.

[13] M. Zolfaghari, M. Abedi, and G. B. Gharehpetian, "Power Flow Control of Interconnected AC–DC Microgrids in Grid-Connected Hybrid Microgrids Using Modified UIPC," IEEE Transactions on Smart Grid, vol. 10, no. 6, pp. 6298-6307, 2019, doi: 10.1109/TSG.2019.2901193.